RESEARCH ARTICLE

Development and Biomechanical Evaluation of an Anatomical 3D Printing Modularized Proximal Inter-Phalangeal Joint Implant Based on the Computed Tomography Image Reconstructions

Yi-Chao Hunag[1,2], Chun-Ming Chang[3], Shao-Fu Huang[2,4], Chia-Heng Hong[2], Chun-Li Lin[2,4]*

[1]Department of Orthopedics and Traumatology, Taipei Veterans General Hospital, Taipei, Taiwan
[2]Department of Biomedical Engineering, National Yang Ming Chiao Tung University, Taipei, Taiwan
[3]Taiwan Instrument Research Institute, National Applied Research Laboratories, Hsinchu, Taiwan
[4]Medical Device Innovation and Translation Center, National Yang Ming Chiao Tung University, Taipei 112, Taiwan

Abstract: In this study, we developed a modularized proximal interphalangeal (PIP) joint implant that closely resembles the anatomical bone articular surface and cavity contour based on computed tomography (CT) image reconstruction. Clouds of points of 48 groups reconstructed phalanx articular surfaces of CT images, including the index, middle, ring, and little fingers, were obtained and fitted to obtain the articular surface using iterative closest points algorithm. Elliptical-cone stems, including the length, the major and minor axis at the stem metaphyseal/diaphyseal side for the proximal and middle phalanxes, were designed. The resurfacing PIP joint implant components included the bi-condylar surface for the proximal phalanx with elliptical-cone stem, ultra-high molecular weight polyethylene bi-concave articular surface for middle phalanx with hook mechanism, and the middle phalanx with elliptical-cone stem. Nine sets of modularized designs were made to meet the needs of clinical requirements and the weakness structure from the nine sets, that is, the worst structure case combination was defined and manufactured using titanium alloy three-dimensional (3D) printing. Biomechanical tests including anti-loosening pull-out strength for the proximal phalanx, elliptical-cone stem, and articular surface connection strength for the middle phalanx, and static/dynamic (25000 cycles) dislocation tests under three daily activity loads for the PIP joint implant were performed to evaluate the stability and anti-dislocation capability. Our experimental results showed that the pull-out force for the proximal phalanx implant was 727.8N. The connection force for the hook mechanism to cone stem of the middle phalanx was 49.9N and the hook mechanism was broken instead of stem pull out from the middle phalanx. The static dislocation forces/dynamic fatigue limits (pass 25000 cyclic load) of daily activities for piano-playing, pen-writing, and can-opening were 525.3N/262.5N, 316.0N/158N, and 115.0N/92N, respectively, and were higher than general corresponding acceptable forces of 19N, 17N, and 45N from the literatures. In conclusion, our developed modularized PIP joint implant with anatomical articular surface and elliptical-cone stem manufactured by titanium alloy 3D printing could provide enough joint stability and the ability to prevent dislocation.

Keywords: Proximal interphalangeal joint; Articular surface; Stem; 3D printing; Biomechanics

1. Introduction

The proximal interphalangeal (PIP) joint is the key actuator for finger motion and function. However, advanced arthritis, including osteoarthritis and inflammatory arthritis, can cause painful disability, joint destruction, and deformity. Conservative treatment, the frontline for symptomatic relief includes oral anti-

inflammatory medication and local injection. For those patients with late stage arthritis that has failed to respond to conservative treatments, joint spacer arthroplasty is one of the surgical strategies to preserve joint motion.

At present, two PIP joint spacer arthroplasty choices that include silicone spacer and joint resurfacing are used in surgical treatment. One-piece silicone implants have been used for decades and have been the gold standard for PIP joint arthroplasty. However, the limitations of PIP joint arthroplasty could be the lack of material rigidity, lateral instability, and the inability to provide force transmission. Furthermore, the fingers cannot bear a forceful pinch[1]. When the joint moves repeatedly and bends under force, the implant is prone to fatigue and fracture. The overall complication rates are as high as 32%[2-4]. The range of motion after silicone implantation is only about 60° compared with 110° in the native joint. This limitation makes it impossible to effectively restore the joint normal range of motion after the operation[5]. On the contrary, metal three-dimensional (3D) printing techniques are well established for building complicated 3D constructions from computer-aided design (CAD) models and have great potential to solve the problems of creating a porous (lattice) surface coating on a dense titanium and porous titanium body[6]. Many studies indicate that titanium implant manufactured by 3D printing with porous design of 60 – 70% porosity and pore size under 800 μm can enhance biologically active and mechanically stable surface for implant fixation to bone[6].

Joint resurfacing (surface replacement) implants were introduced and commonly used in the last two decades. Various designs with different materials are available on the market. Surface replacement arthroplasty has better structural strength and biomechanical performance compared with silicon arthroplasty, providing a larger range of joint activities. However, the shape and size of the stem mismatch with the bone marrow cavity size and the lack of osseointegration makes the implant prone to loosening under repetitive force. This leads to implant failure and the need for a second operation in symptomatic patients[2]. Commercially available products have articular surfaces that do not resemble the natural articular surface shape. This results in unstable joint arc motion and easy joint dislocation[5,7]. These factors present a large challenge and time consuming because it involves traditional machine manufacturing processes to fabricate the small PIP joint implant. The implant stem elliptical cross-section must completely fit into the medullary cavity, matching the complex anatomical bimodal shape of the articular surface to prevent dislocation.

In current clinical practice, most finger joint implants were designed in accordance with simplified size specifications. However, PIP joint implant restricted specifications and sizes may not be suitable for various patients due to racial and individual diversity. Further, the design of PIP joint implant needs to be adjusted to establish a modularized PIP joint implant with suitable implant stem and articular surface size combinations that can meet the clinical use of various patients[8]. Therefore, developing a modularized implant that consistently preserves PIP joint stability with appropriate stem fitness for the bone marrow cavity with relative natural articular surface shape for long-term durability is needed. A new manufacturing process is required for such an implant device.

This study developed a modularized PIP joint implant system that closely resembles the anatomical articular resurfacing and stem based on reconstructed computed tomography (CT) images using the iterative closest points approach. Each component of the newly designed PIP joint with complex geometric shapes was fabricated through metal 3D printing. Biomechanical tests including anti-loosening pull-out strength for the proximal phalanx, elliptical-cone stem, and articular surface connection strength for the middle phalanx, and static/dynamic dislocation tests under three daily activity load conditions for the PIP joint implant were performed to verify joint stability and dislocation reduction.

2. Materials and methods

2.1. PIP joint implant design concept

The PIP joint is a hinge joint with a bicondylar-shaped proximal phalangeal head articulating with the bi-concave-shaped middle phalangeal base. It is stabilized with collateral ligaments and the volar plate, providing a motion arc of about 110° in flexion-extension. Therefore, our joint design concept is to resemble the anatomical contours and structure as closely as possible. Modularized models of the metaphyseal stem and joint surface replacement provide diverse combinations for proper fit of a wider variety of human fingers.

In terms of the PIP joint implant design, a total of 48 CT image sets (Aquilion Prime SP, Canon Medical Systems USA, Inc., CA, US) including the index finger, middle finger, ring finger and little finger were obtained from 12 patients (including seven males and five females) aged between 20 and 65 years old. We obtained the CT files from the Picture Archiving and Communication System by the location of exam at wrist and fingertips of all digits. Any suspicions or findings of injury or arthritic change were excluded from the study. Ethic approval was not applied in this study since all patients' demographic data were not revealed. CT images were reconstructed to measure the size, shape of the metaphyseal, diaphyseal, and medullary cavity at both proximal and middle phalanxes in medical image processing software (Mimics 22.0, Materialize NV, Leuven, Belgium).

For the PIP joint implant stem design, the measured total length of the phalanx minus the resection thickness of the cut ends was defined as the full length of phalangeal bone marrow because the planned resection thickness was 4 mm for the proximal phalangeal articular surface and 2 mm for the middle phalangeal articular surface to remove the worn cartilage. One-third of the full length of bone marrow cavity, which was designed for part of adequate metaphyseal contact surface for bone integration and part of press fit for diaphyseal portion, was defined as the length for the modularized stem (**Figure 1A**). Lengths in the medullary cavity sagittal plane and coronal plane cross section were measured and noted as the minor axis and major axis for the elliptical medullary cavity (**Figure 1B**). A total of 48 sets of measurements were averaged to find the implant stem dimensions, including the length, the major and minor axis of the metaphyseal and diaphyseal sides of the proximal phalanx and middle phalanx stems (**Figure 1B**).

PIP joint surface design and articular surface border were defined according to the extensor tendon and ligaments insertion sites. The joint was retained with 135° articular curved surface. Clouds of points from 48 groups of reconstructed phalanx articular surfaces were fitted
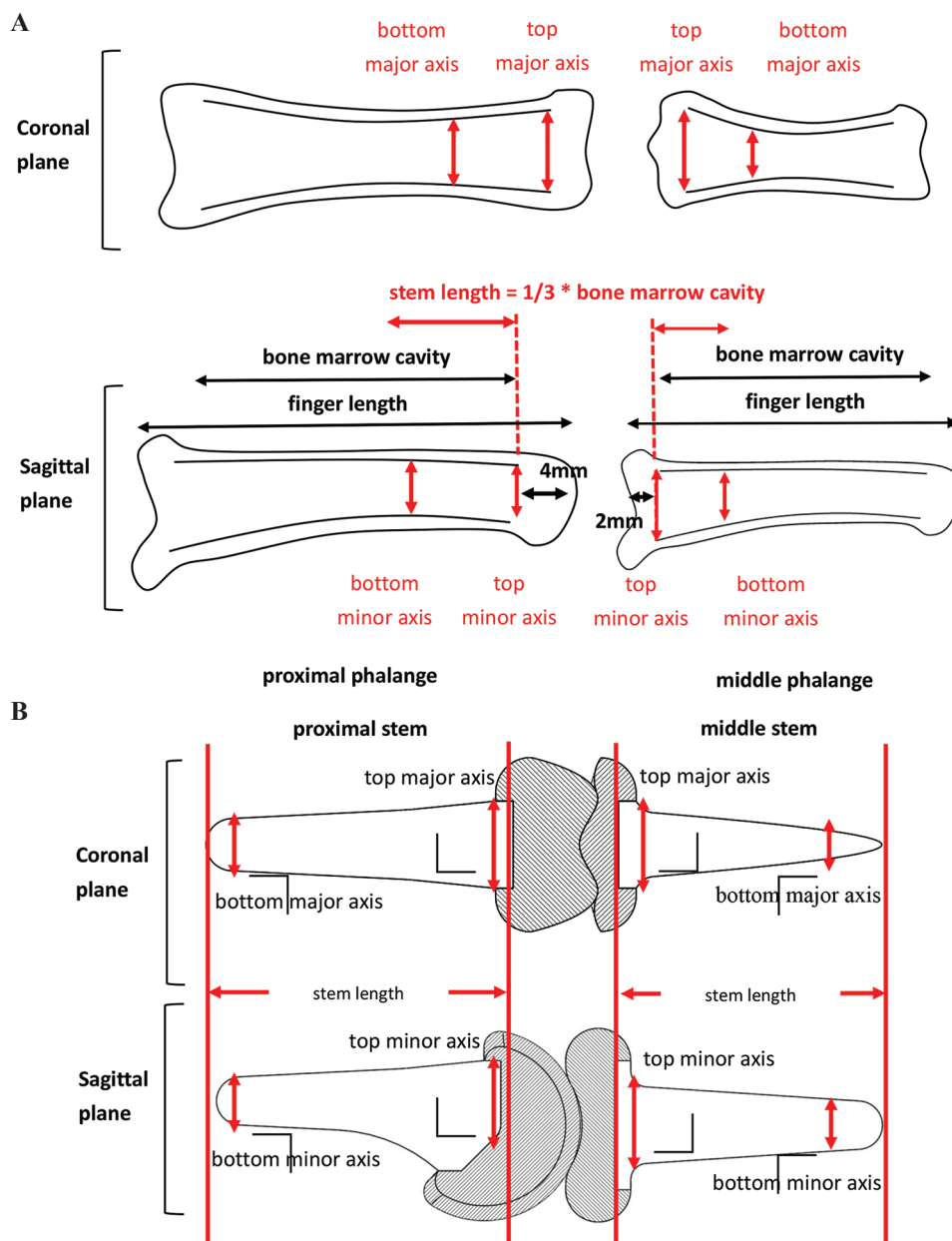

Figure 1. PIP joint implant design concept: medullary canal estimation and stem length.

into the natural articular surface using the iterative closest points (ICP) algorithm provided in the Mimics software. The calculation formula is shown in[9]:

$$E\left(R, T\right) = \sum_{i=1}^{n} ((R*pi + T) - qi)2$$

where pi is the point cloud coordinates for the alignment model P, qi is the point cloud coordinates for the target alignment model Q, *n* is the number of reference point clouds (*n* = 1000), R is the rotation matrix, and T is the translation matrix. Each iteration is intended to calculate the distance between the point cloud pi coordinates for the alignment model and the point cloud qi coordinates for the target alignment model after matrix transformation. The iteration was stopped when the difference between the front and rear transformation matrices is less than the set threshold value. This iteration process enabled phalanges of different sizes to align with the large shared volume. Natural articular surfaces in the clinical representatives were obtained by averaging the coordinates from the 48 aligned point clouds of phalanx articular surfaces (**Figure 2A**).

2.2. Modularized PIP joint implant system design and worst structure case definition

The components for resurfacing the PIP joint implant include three parts, bi-condylar surface with elliptical-cone stem of proximal phalanx, the bi-concave articular surface of middle phalanx, and the elliptical-cone stem of middle phalanx. The bi-concave articular surface was designed to connect with the elliptical-cone stem using a hook mechanism (**Figure 2B and C**).

The averaged stem lengths (12 mm for proximal stem and 7.5 mm for middle stem), major and minor axis of the elliptical-cone stem at metaphyseal and diaphyseal for proximal and middle phalanxes were calculated from the 48 sets of phalanx CT image data and noted as the standard size specification (**Figure 2B and C**). Since the size of 20% above/below the standard PIP joint implant size was about the average dimension plus/minus 1.3 standard deviation, covering about 80% of the 48 phalanges' size. The size was set at 20% above and below the averaged standard size as the maximum and minimum sizes, respectively. An intermediate size of 10% was inserted to cover the entire PIP joint implant detailed size range. Finally, a total of five sizes for the PIP joint implant, consisting of 20%, 10%, standard size, −10% and −20%, were considered (**Table 1**). There were five specifications for both the articular surfaces and the cone stems for proximal and middle phalanxes, which in free combination would make up 25 sets of modularized specifications.

Considering the more plausible combination of the stem and articular surface of anatomical proportion, the modularized PIP joint implant with the stem smaller and greater than the joint surface over two levels were excluded, leaving the modularized PIP joint implant the modularized with the same size and the joint surface greater than one level of the stem. From the anatomical and clinical consideration, the medullary cavity could be occasional smaller due to thick metaphyseal of diaphyseal cortical bone. However, mismatch with large medullary cavity with smaller articulation was seldom observed, which may affect the range of motion of joint. Under such conditions there were a total of nine sets of specifications (**Table 1**).

For the subsequent functional biomechanical test requirements, it was necessary to determine the combination of nine PIP joint implant specification sets with the weakest structure after the PIP joint was implanted with the phalanx. When the medullary cavity ratio to the entire phalanx cross-sectional areas was largest, that is, the one with the smallest cortex bone thickness was defined as the weakest state structure. A structural weakness combination from the nine PIP joint implants can be found using the following three steps: (i) the phalanges with the largest size, medium size (averaged size) and the smallest size among the 48 phalanges were screened; (ii) corresponding medullary cavity ratio to the cross-sectional area at the phalanx stem top and bottom sides of the previous largest and medium sizes were obtained and these sizes were recorded to find the phalange with maximum ratio, that is, the PIP joint with the thinnest cortex bone case; and (iii) the combination of nine groups of PIP joint implants that can be put into the case of the thinnest cortex bone with the largest stem size was checked. Furthermore, a larger force state can be generated when the articular surface level was larger than the corresponding stem level combination. Therefore, the structural weakness combination from the nine PIP joint implants can be found and defined as the worst structure case. This combination was used for functional mechanical test to observe the biomechanical performance of modularized pairing under different specifications.

2.3. 3D printing manufacture of the worst PIP joint implant

The proximal phalangeal stem and articular surface components as well as the middle phalangeal stem were fabricated by metal 3D printer (AM400, Renishaw, Gloucestershire, UK) with titanium alloy powder (about 30 μm), which had been proved with good biocompatibility and was also used widely in clinical practice. Our 3D printer laboratory was approved by ISO13485 quality management system (Certificate Number: 1760.190828) to ensure that implants manufactured by 3D printing can provide a practical foundation to meet the regulations, such as printing material with biocompatibility in the
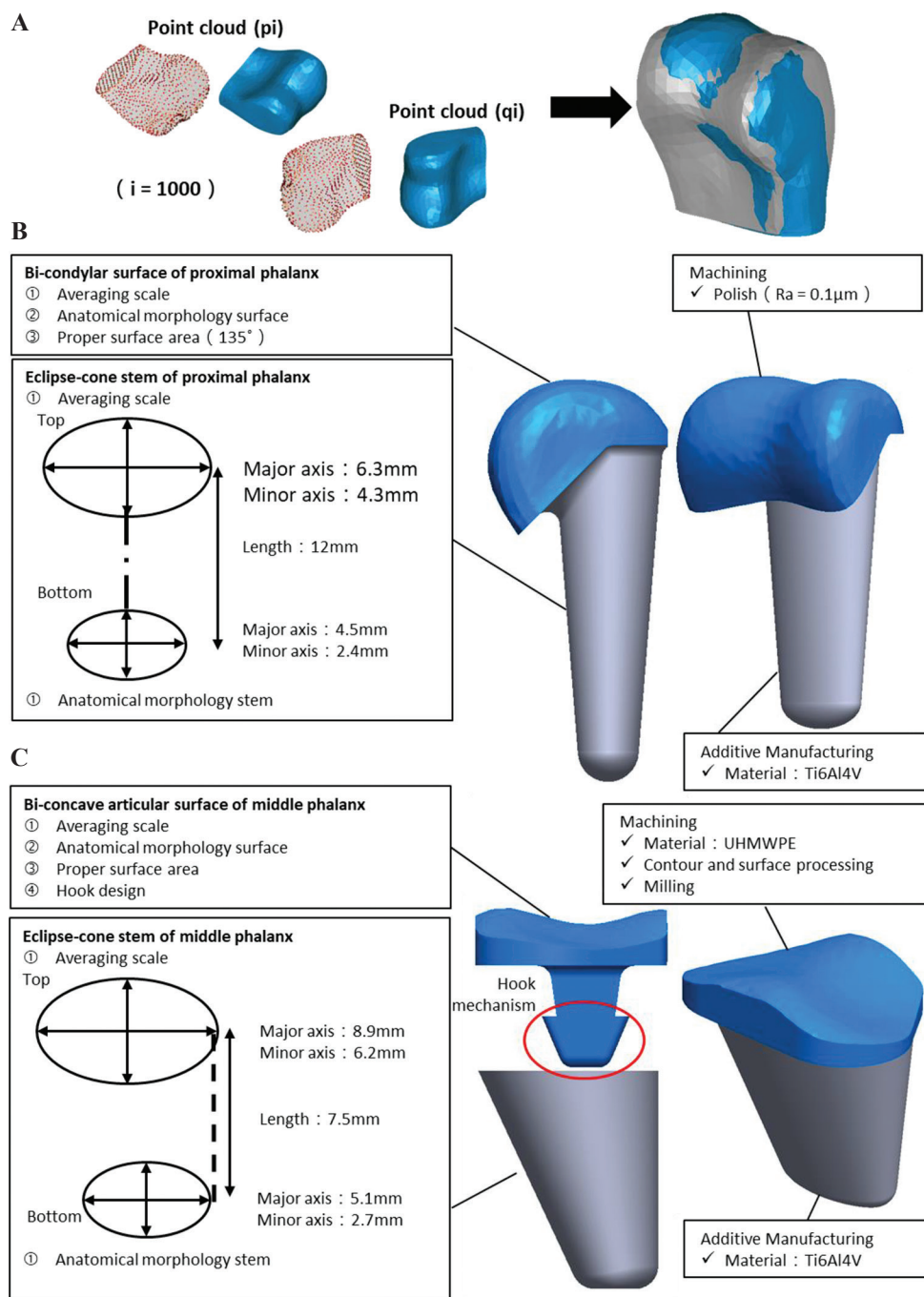
Figure 2. (A) Native articular surface was obtained from 48 aligned point clouds using iterative closest points (ICP) algorithm; (B and C) Design dimension of our PIP joint implant: elliptical-cone stem, bi-condylar metal surface and bi-concave UHMWPE.

context of biological safety to meet ISO10993 standard as well as demonstrating a commitment to the safety and quality. After 3D printing, all components were acid-etched to remove residual sandblast particles and cleaned using ultrasonic oscillations[10]. To reduce the frictional resistance of the joint surface movement, the proximal articular surface was subjected to polishing and the surface roughness value Ra was controlled to be < 0.1 μm. The articular surface component with

hook mechanism for the middle phalanx was made of ultra-high molecular weight polyethylene (UHMWPE) and manufactured by machine milling **(Figure 2C)**. The manufacturing accuracy was compared with the design sizes to fabricate product dimensions (elliptical cross-section and the total length of the proximal and middle phalanx stems) using the SVP manual imaging measurement system (Arcs Precision Technology Co., LTD, Taipei, Taiwan).

2.4. Functional biomechanical testing

The biomechanical testing of the remaining bone model for PIP joint implant insertion was performed using the standard size specification solid digital proximal and middle phalanx models with articular surface resection. The digital phalanx models were duplicated in acrylonitrile butadiene styrene (ABS-P430; Strayasys, Ltd., Minnesota, USA) using a 3D printer (Dimension 1200es SST, Strayasys, Ltd., Minnesota, USA) to mimic the bone material[10]. There were three biomechanical tests including (i) anti-loosening pull-out test of PIP joint for proximal phalanx; (ii) elliptical-cone stem and articular surface connection strength of the middle phalanx; and (iii) dislocation test under three daily PIP joint implant activity load conditions. Tests were performed to verify joint stability and ability.

To assess the anti-loosening ability of the proximal stem design, the pull-out testing was performed under a hand-held 4.5 kgw weight applied on the PIP joint according to the study by Butz[11]. Three PIP joint proximal stems were inserted into the corresponding ABS proximal phalanxes and the proximal one-third of the phalanx was embedded into a resin block and clamped onto the test machine (HT-2402EC, Hung Ta Instrument, LTD, Taichuang, Taiwan) (**Figure 3A and B**). While, another C holding device connected to a load cell was applied to clamp both palmar and dorsal sides of the proximal PIP joint to perform the pull-out test with a constant vertical upward force at the speed of 5mm/min. The maximum pull-out force was recorded to determine the retention between the PIP joint implant and proximal phalanx.

To evaluate the hook mechanism connection force between the bi-concave articular surface and middle phalanx elliptical-cone stem, the simplified articular surface (plate) with hook mechanism connected to the 3D printing cone stem was inserted into the corresponding ABS middle phalanx marrow cavity and clamped onto the test machine. A specifically designed load device with two cylinders were applied onto both edges of the simplified articular surface (plate) to perform the pull-out testing under the same hand-held weight with 4.5 kgw and loading speed (**Figure 3C and D**). The pull-out test was stopped when the pull-out force suddenly dropped, the hook mechanism or the cone stem was pulled out. The maximum pull-out force and failure mode were recorded.
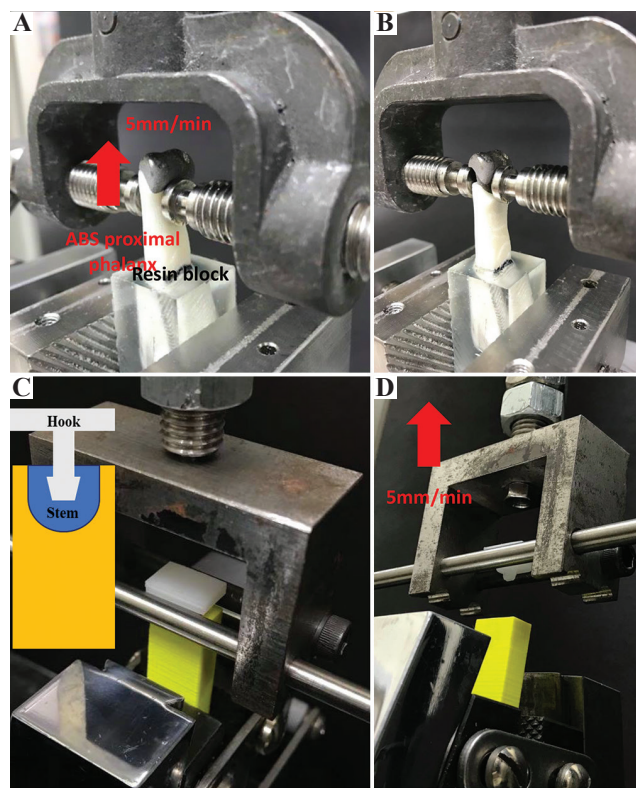
To test the anti-dislocation ability of our PIP joint implant, piano-playing and pen-writing motions according to the work of Butz[11], and the can-opening action were applied as the load conditions to evaluate PIP joint implant dislocation in static and dynamic tests[12]. The dislocation test setup was similar to that of Completo in which the PIP joint at the proximal phalanx was embedded into a block and connected to the testing machine load cell (Instron, E10000, INSTRON, Canton, MA, USA)[13]. The corresponding PIP joint at the middle phalanx was also embedded and fixed into an adjustable angle clamp (**Figure 4A and B**).

The applied forces with angle of 25°, 35° and 55° of the clamp were mimicked to the previously

Table 1. Specifications of 9 sets of modularized PIP joint implants.


Figure 3. (A and B) Anti-loosening pull-out test for PIP joint for proximal phalanx; (C and D) Pull-out testing for hook mechanism connection strength between UHMWPE and middle phalanx stem.

daily motions of piano-playing, pen-writing, and can-opening. The test setup was needed to ensure joint surface alignment and full contact (**Figure 4C**). The static dislocation test was performed by applying vertical downward compressive force at a constant speed of 5 mm/min on the implant, which was stopped when the load dropped or the joint surface became misaligned. The maximal dislocation force and the damage situation were recorded and compared with the results from the previous literatures.

Regarding the dynamic test, cyclic force sine wave mode at 1 Hz frequency was performed for a total of 25,000 cycles to simulate the normal joint activity 1 month after the operation[13]. The force was initiated at 50% of the maximum dislocation force in the corresponding three static tests. Force was then increased at a gradient of 10% until the cyclic load limit number was obtained maximum 25,000 cycles (cannot pass 25,000 cycles). Three samples from each set were used to obtain the corresponding percentages for three static loads with different angles. The misalignments were then observed and recorded.

3. Results

The medullary cavity ratio to the cross-sectional area at the phalanx stem top and bottom sides of largest,
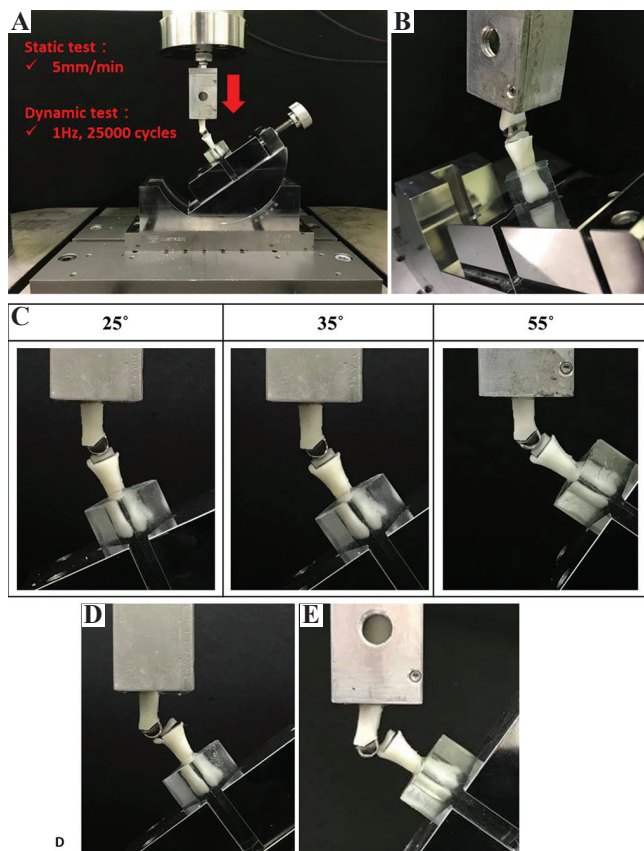
Figure 4. Tests of anti-dislocation ability for PIP joint prosthesis at 25°, 35°, 55°and on failure mode.

medium, and smallest phalanges were ranged from 30% to 72%, of which 72% occurs at the metaphyseal of the largest phalanx size (**Table 2**). In addition, there were 5 PIP joint implant combination sets, that is, 0% (articular surface) to 0% (stem), 10% (articular surface) to 0% (stem), 10% (articular surface) to 10% (stem), 20% (articular surface) to 10% (stem), and 20% (articular surface) to 20% (stem) that can be placed into this largest phalanx. Finally, the worst structure case, that is, weakest structure in all set combinations was the enlarged 20% of the articular surface and 10% of the stem size due to the articular surface level was larger than the corresponding stem level combination to produce a larger force state (**Table 2**).

Figure 5A shows the PIP joint implant including 3D printing proximal phalanx with polished articular surface and middle phalanx consisting of 3D printing cone stem and milling UHMWPE curved articular surface connected by hook mechanism. The major axis and minor axis of the metaphyseal and diaphyseal ellipses and the total length of the stem for proximal and middle phalanxes were recorded. The error percentages were all within ±5% compared with the CAD design value (**Tables 3 and 4**).
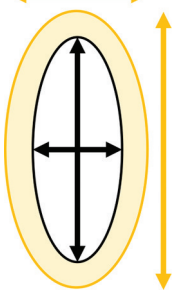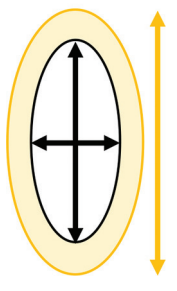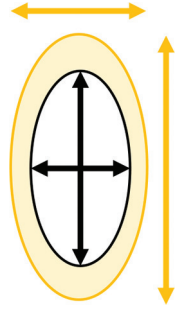
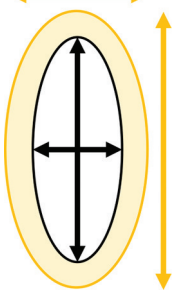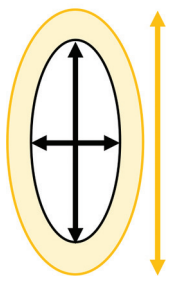The maximum pull-out force of the proximal phalanx prosthesis was 727.8N ± 45.6N (average value ± standard deviation) and the loosening failure mode is shown in **Figure 4B**. The maximum connection force of the hook mechanism to cone stem of the middle phalan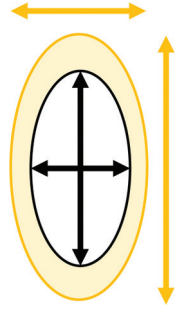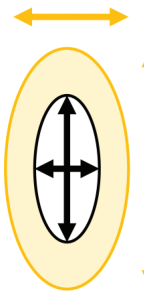x is 49.9N ± 2.0N (average value ± standard deviation) and the hook mechanism was broken instead of cone stem pull-out from middle phalanx in **Figure 3D**.

The dislocation force of 25°, 35°, and 55° for PIP joint implant were 525.3N ± 21.2N, 316.0N± 17.2N, and 115.0N ± 1.8N, respectively (**Table 5**) and **Figure 6** shows the load displacement diagram of all dislocation tests. **Figure 4D** shows the dislocation situation under 35° load condition and fractured bone around the UHMWPE articular surface of the middle phalanx was found. Corresponding percentages of three static loads with different angles that can pass 25000 dynamic cyclic loads were 50% (26.25~262.5N), 50% (15.8~158N), and 80% (9.2~92N) for 25°, 35°, and 55° load conditions, respectively (**Table 6**). **Figure 6E** shows the misalignment of the PIP joint implant under 55° dynamic load cycles.

4. Discussion

Although PIP joint arthroplasty is well-established, it can still be a challenging task for surgeons[1,2]. Current commercial artificial PIP joint implants have the following limitations; one-piece silicone implants lack appropriate rigidity, resulting in lateral instability and weak pinch, and implant breakage due to repetitive usage[1-4]. Although

Table 2. The ratios of the medullary cavity and stem cross-sectional area.

Worst structure case	Max. size of phalanx	Middle size of phalanx	Min. size of phalanx
72%	Top Major axis: 72% Minor axis: 40%	Top Major axis: 65% Minor axis: 52%	Top Major axis: 57% Minor axis: 70%
0% (articular surface) to 0% (stem) 10% (articular surface) to 0% (stem) 10% (articular surface) to 10% (stem) 20% (articular surface) to 10% (stem) 20% (articular surface) to 20% (stem)	Bottom Major axis: 48% Minor axis: 30%	Bottom Major axis: 47% Minor axis: 35%	Bottom Major axis: 37% Minor axis: 37%
5 sets can be placed in this largest phalanx			

Left column: worst case definition; right three columns: ratios of the medullary cavity and the cross-sectional area at stem top and bottom sides of the phalanx for largest, medium size (averaged size) and the smallest size among the 48 phalanges

joint resurfacing arthroplasty produces better motion arc, structural strength, and biomechanical performance, symmetrical condyles over a range of sizes for all the fingers compromise the natural finger joint alignment. Faced with clinically diverse patients with individual differences, joint implants with a single specification cannot adapt to various anatomical types. Articular surface and fixating stem mismatch to the bone marrow cavity and the inadequate osseointegration to higher incidence of implant loosening.

This study designed modularized 3-part components, including bicondylar surface, bi-concave articular surface, and elliptical-cone stem according to the CT image data base. The modularized condylar components were fabricated using metal 3D printing technique which can achieve a tolerance of <5% under complex PIP joint shapes. The modularized implant design can provide better compliance in current clinical practice with consistent joint stability with worthy stem fitness in bone marrow cavity and long-term durability.
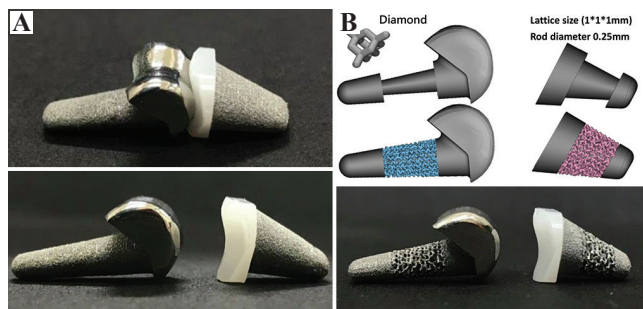
Considering the time and cost-effectiveness of functional mechanical testing, it is necessary to select a group of the clinically most dangerous modularized from the nine groups of standard modularized

Figure 5. (A) 3D printing modularized PIP joint prosthesis; (B) 3D printing lattice with 0.8mm thickness, length of 6 mm for proximal phalanx stem and 4 mm for middle phalanx stem in our PIP joint prosthesis to promote bone growth.

for experimentation. The combination of stem modularized components with an additional 10% in size and the articular surface with an additional 20% in size were chosen. Larger articular surfaces lead to a larger stress area in the joints and the overall joint and phalanx stress is also large. If the most dangerous modularized meets the acceptable standard through the experimental results, the remaining eight groups of modularized can meet the acceptable functional mechanical test standard.

About functional biomechanical testing, the phalanx models were duplicated in ABS using a 3D printer to mimic the bone material for resurfacing prosthesis implantation. To uniformly simplify the material and anatomical phalangeal bone, although ABS material is quite different from the real bone material, the functional biomechanical tests were able to show a reference trend according to similar bone contours. Similar methods were also applied in many literatures[10,14].

Butz simulated a hand-held 4.5 kgw weight[11], the proximal joint received a force of 84N at a 60° angle and the vertical component force at the articular surface was 42N (noted as the standard force). The proximal phalanx PIP joint anti-loosening pull-out test showed that the average maximum pull-out force was 727.8N, and it was as high as 17 times compared to the standard force. The corresponding value of the medial articular UHMWPE surface with hook mechanism was 49.9 ± 2.0N, which was also higher than the standard force. In addition, the middle 3D printing phalanx was not extracted, indicating that the retention strength between middle phalanx and ABS bone was enough. These results demonstrate that the elliptical-cone stem of our PIP joint can provide good anti-loosening ability under the force of daily activities.

Concurrent joint prostheses commonly used a combination of metal on polymer or pyro carbon and demonstrated low friction and wear. Due to our good performance of anti-loosening and anti-pull-out test of

Table 3. The product dimension, design dimension and error percentages of major axis and minor axis of the metaphyseal and diaphyseal ellipses and the total length of the stem for proximal phalanxes.

Proximal stem	Top major axis	Top minor axis	Bottom major axis	Bottom minor axis	Stem length
Measurement	6.89±0.05	4.90±0.05	4.80±0.01	2.60±0.04	13.44±0.02
Design	6.93	4.73	4.95	2.64	13.20
Error (%)	−0.52	3.66	−3.12	−1.65	1.84

Table 4. The product dimension, design dimension and error percentages of major axis and minor axis of the metaphyseal and diaphyseal ellipses and the total length of the stem for middle phalanxes.

Middle stem	Top major axis	Top minor axis	Bottom major axis	Bottom minor axis	Stem length
Measurement	9.68±0.03	6.83±0.06	5.37±0.05	2.91±0.03	8.56±0.02
Design	9.79	6.82	5.61	2.97	8.25
Error (%)	−1.09	0.18	−4.24	−2.00	3.86

Table 5. The dislocation force of 25°, 35° and 55° for PIP joint implant.

Angle	S1	S2	S3	Mean±SD
25°	549.8N	513.0N	513.4N	525.3±21.2N
35°	335.5N	309.5N	303.0N	316.0±17.2N
55°	117.0N	114.1N	113.8N	115.0±1.8N

Table 6. Static strength and capable percentage of 25000 dynamic cyclic loads with different angles.

Angle	Static Strength	Dynamic Fatigue Loading (%)
25°	525.3±21.2N	50 (26.25~262.5N)
35°	316.0±17.2N	50 (15.8~158N)
55°	115.0±1.8N	80 (9.2~92N)
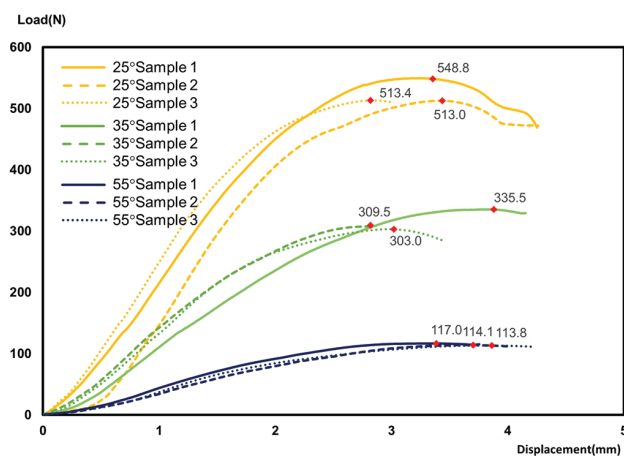
Figure 6. Load-displacement diagram of dislocation tests.

the modularized PIP joint implant showed in this study. Hence, we chose a commonly used combination of metal on polymer. The main reason of using UHMWPE was its broad utility in current large joint arthroplasty, including hip, knee, ankle, and shoulder joint arthroplasty, as well as its good ability of decreasing the bearing surface wear and avoids debris or particles that induce third-body wear. Otherwise, the cross-linked polyethylene had not only shown superior results compared with previous polymer-on-polymer, such as UHMWPE but also a wear rate comparable to metal-on-polymer combinations[15,16]. Cross-linked polyethylene was also able to be fabricated by injection molding manufacturing to reduce production costs. Cross-linked polyethylene was proposed as the articular surface of the middle phalanx and contact movement with 3D printing polished articular surface of the proximal phalanx for our PIP joint resurfacing prosthesis.

In many common finger joint movements in daily life, such as playing the piano, writing with a pen and open a can, the magnitude and angle of the joint force are well known[11,12]. The joints are subjected to a force

of 19N at a 25° angle under the action of playing the piano. The joint receives a force of 17N at a 35° angle when holding the pen under writing action and the joint receives a force of 45N at a 55° angle while opening a can. The dislocation test result under three daily activity load conditions showed that the dislocation force values for the three stress degrees were much higher than those normal joint force values with different actions. The dislocation force decreased reasonably with larger joint angle but produced maximum misalignment. The fatigue force ratio of misalignment to the literature data was set as the safety factor. The fatigue limit of the 25°, 35°, and 55° groups was 262.5N, 158N, and 92N, respectively. The corresponding three safety factors were about 14 (262.5N/19N), 9 (158N/17N), and 2 (92N/45N). This was found at least more than twice the static acceptance condition and addressed that the articular surface design of our PIP joint can provide good anti-dislocation ability under the force of daily activities.

The stem fixation methods are mechanical, cement, and bone ingrowth. Due to the smaller PIP joint size, the type of fixation depends mainly on the bone stock condition, which was often interfered with by the severity of arthritis. Therefore, cement or mechanical fixation was often difficult and impractical. Our modularized elliptical cone shape stem aimed to provide adequate contact area and force between the metal and phalangeal bone and decreases the stress-relaxing properties by further bone resorption, which reduces implant loosening and fracture.

To optimize the osseointegration ability and delaminate implant loosening, additive manufacturing with enhancement of cell-biomaterial interactions is an attractive option since it is able to meet biological and functional demands. To optimize the osseointegration ability and delaminate implant loosening, additive manufacturing with enhancement of cell-biomaterial interactions draw attention and is able to meet biological and functional demands[6]. 3D structured material that comprises a lattice design was adopted on the metaphysis surface to promote bone ingrowth. The constructs at distinctive well-defined range of length scales and parameter magnitudes are expected to differentially affect on cellular and surface interaction of osseointegration. Hara *et al*. (2016) mentioned that metal-interfaced implants with diamond-structured porous titanium-alloy (Porous Ti-alloy) can promote osseointegration and enhance implant stability[17]. The most important parameters that affect osseointegration are pore size and porosity. The experimental group with a size of 640 μm and a porosity of 70% had better bone tissue growth ability and the strongest mechanical performance. We already have the technology to design and fabricate this type of lattice on the elliptical-cone stem surface (0.8 mm

thickness and a specific length of 6 mm for proximal side and 4 mm for middle side) in our PIP joint to promote bone growth (**Figure 5B**). However, this technology needs to be tested in future in vivo experiments because the surface lattice design used in this *in vitro* anti-loosing pull-out test could not portray the function of bone growing into the lattice.

In the design of our PIP joint, only 48 sets of CT images of the hand were collected based on the image reconstruction samples of 12 patients to establish the appearance of the anatomical articulation and modularized specification definition. Perhaps, more sets of image augmentation databases should be included to establish a design closer to the natural joint shape and contour in the future. The phalanx model for these functional mechanical experiments was a hot-melt stacked ABS material. It utilized cadaver bone and cannot simulate osseointegration. The load and boundary fixing method of the experimental setup was a simplified clinical situation, which was different from the actual situation, and the result was only for trend reference.

5. Conclusion

We successfully developed a modularized PIP joint implant which resembles the anatomical shape and an elliptical-cone stem based on CT image reconstruction. Complex geometry of each PIP joint component can be fabricated by 3D printing technology with traditional mechanical polishing. Results of biomechanical tests encompassing static pull-out test, buckle mechanism test, functional static and dynamic dislocation tests indicate that our novel PIP joint implant reaches a certain joint stability and ability to prevent dislocation under simulated daily hand use activities.

Funding

Conflict of interest

The authors declare no conflicts of interest.

Author contributions

C.L.L supervised this study and revised the article of this manuscript. Y.C.H designed and supervised the development of PIP joint prosthesis and wrote manuscription. Y.C.H, C.M.C, S.F.H, and C.H.H, conducted experiments and contributed intellectually to the scientific design of the functional biomechanical testing, C.M.C mentored the technical part of the project.

References

1. Yamamoto M, 2017, A Systematic Review of Different Implants and Approaches for Proximal Interphalangeal Joint Arthroplasty. *Plast Reconstr Surg*, 139:1139e–51.
   https://doi.org/10.1097/prs.0000000000003260

2. Lans J, 2019. Factors Associated with Reoperation after Silicone Proximal Interphalangeal Joint Arthroplasty. *Hand*, 15:674–8.
   https://doi.org/10.1177/1558944719864453

3. Srnec JJ, 2017, Implant Arthroplasty for Proximal Interphalangeal, Metacarpophalangeal, and Trapeziometacarpal Joint Degeneration. *J Hand Surg Am*, 42:817–25.
   https://doi.org/10.1016/j.jhsa.2017.07.030

4. Bales JG, 2014, Long-Term Results of Swanson Silicone Arthroplasty for Proximal Interphalangeal Joint Osteoarthritis. *J Hand Surg Am*, 39:455–61.
   https://doi.org/10.1016/j.jhsa.2013.11.008

5. Selig HF, 2020, Outcome of Proximal Interphalangeal Joint Replacement with Pyrocarbon Implants: A Long-Term Longitudinal Follow-up Study. *Arch Orthop Trauma Surg*, 140:1847–57.
   https://doi.org/10.1007/s00402-020-03592-3

6. Zaeri A, Cao K, Zhang FC, *et al.*, 2022, A Review of the Structural and Physical Properties that Govern Cell Interactions with Structured Biomaterials Enabled by Additive Manufacturing. *Bioprinting*, 26:e0020.
   https://doi.org/10.1016/j.bprint.2022.e00201

7. Aversano FJ, 2018, Salvaging a Failed Proximal Interphalangeal Joint Implant. *Hand Clin*, 34:217–27.
   https://doi.org/10.1016/j.hcl.2017.12.011

8. Griffart A, 2019, Arthroplasty of the Proximal Interphalangeal Joint with the Tactys Modular Prosthesis: Results in Case of Index Finger and Clinodactyly. *Hand Surg Rehabil*, 38:179–85.
   https://doi.org/10.1016/j.hansur.2019.03.001

9. Ying H, 2017, An Iterative Closest Points Algorithm for Registration of 3D Laser Scanner Point Clouds with Geometric Features. *Sensors*, 17:1862.
   https://doi.org/10.3390/s17081862

10. Li CH, Wu CH, Lin CL, 2020, Design of a Patient-Specific Mandible Reconstruction Implant with Dental Prosthesis for Metal 3D Printing Using Integrated Weighted Topology Optimization and Finite Element Analysis. *J Mech Behav Biomed Mater*, 105:103700.
    https://doi.org/10.1016/j.jmbbm.2020.103700

11. Butz KD, 2012, A Biomechanical Analysis of Finger

Joint Forces and Stresses Developed during Common Daily Activities. *Comput Methods Biomech Biomed Eng*, 15:131–40.

https://doi.org/10.1080/10255842.2010.517525

12. Purves WK, 1980, Resultant Finger Joint Loads in Selected Activities. *J Biomed Eng*, 2:285–9.

13. Completo A, 2018, Biomechanical Evaluation of Pyrocarbon Proximal Interphalangeal Joint Arthroplasty: An *In-Vitro* Analysis. *Clin Biomech*, 52:72–8.

https://doi.org/10.1016/j.clinbiomech.2018.01.005

14. Lin CL, Wang YT, Chang CM, *et al*., 2022, Design Criteria for Patient-specific Mandibular Continuity Defect Reconstructed Implant with Lightweight Structure using Weighted Topology Optimization and Validated with Biomechanical Fatigue Testing. *Int J Bioprint*, 8:437.

https://doi.org/10.18063/ijb.v8i1.437

15. Stokoe S, 1990, A Finger Function Simulator and Surface Replacement Prosthesis for the Metacarpo-Phalangeal Joint. PhD Thesis, University of Durham.

16. Joyce TJ, Ash HE, Unsworth A, 1996, The Wear of Cross-linked Polyethylene Against Itself. *Proc Inst Mech Eng H*, 210:11–6.

https://doi.org/10.1243/pime_proc_1996_210_386_02

17. Hara D, Nakashima Y, Sato T, *et al*., 2016, Bone Bonding Strength of Diamond-structured Porous Titanium-alloy Implants Manufactured Using the Electron Beam-melting Technique. *Mater Sci Eng C*, 59:1047–52.

https://doi.org/10.1016/j.msec.2015.11.025

Publisher's note